

## Influence of Substituents on the Energy and Nature of the Lowest Excited States of Heteroleptic Phosphorescent Ir(III) Complexes: A Joint Theoretical and Experimental Study

Igor Avilov,<sup>\*,†</sup> Payam Minoofar,<sup>‡</sup> Jérôme Cornil,<sup>\*,†</sup> and Luisa De Cola<sup>‡</sup>

Contribution from the Service de Chimie des Matériaux Nouveaux, Université de Mons-Hainaut, Place du Parc 20, B-7000 Mons, Belgium, and Westfälische Wilhelms Universität Münster, Mendelstrasse 7, D-48149 Münster, Germany

Received February 24, 2007; E-mail: Jerome@averell.umh.ac.be; avilovi@averell.umh.ac.be

**Abstract:** A series of Ir(III)-based heteroleptic complexes with phenylpyridine (ppy) and 2-(5-phenyl-4H-[1,2,4]triazol-3-yl)-pyridine (ptpy) derivatives as coordinating ligands has been characterized by a number of experimental and theoretical techniques. Density functional theory (DFT) calculations were able to reproduce and rationalize the experimental redox and excited-states properties of the Ir complexes under study. The introduction of fluorine and trifluoromethyl substituents is found not only to modulate the emission energy but also often to change the ordering of the lowest excited triplet states and hence their localization. The lowest triplet states are best characterized as local excitations of one of the chromophoric ligands (ppy or ptpy). The admixture of metal-to-ligand charge-transfer (MLCT) and ligand-to-ligand charge-transfer (LLCT) character is small and strongly depends on the nature of the excited state; their role is, however, primordial in defining the radiative decay rate of the complexes. The extent of charge-transfer contributions depends on the energy gaps between the relevant molecular orbitals, which can be modified by the substitution pattern.

### 1. Introduction

During the past decade, a great interest has been devoted to the development of organic light-emitting diodes (OLEDs) for application in the next generation of flat panel displays and conventional lighting. Currently, a significant amount of the LED research is devoted to small molecule phosphorescent LEDs.

Phosphorescent emitters that contain a heavy metal center possess an advantage over fluorescent emitters with their strong spin-orbit coupling induced by the presence of the heavy metal atom. This spin-orbit coupling allows for harvesting both triplet and singlet excitons due to efficient intersystem crossing processes. Thus, the internal quantum efficiency in electrophosphorescent devices can approach 100%.<sup>1–4</sup> In this context, various complexes of Ir(III) are particularly promising in view of their high luminescence efficiency.<sup>5–7</sup>

An important challenge is to design efficient phosphorescent dopants to emit the three primary colors (i.e., red, green, and blue). To do so, the most common approach is to graft various electron-withdrawing or electron-donating substituents at different positions of the coordinated ligands.<sup>6,8–14</sup> A success in the development of efficient emitters for full-color displays depends to a great extent on the knowledge of the nature of the emissive excited states. One important issue is the extent of mixture of ligand-centered (LC) and metal-to-ligand charge transfer (MLCT) characters in the excited states of the complexes. We will show hereafter that a larger amount of MLCT character in the lowest singlet and triplet states leads to a smaller energy gap ( $\Delta E_{ST}$ ) between them, thus increasing the degree of mixing of singlet *versus* triplet character. In turn, this leads to a larger radiative decay rate, as suggested in refs 15–18. In addition, a higher degree of admixture of MLCT character

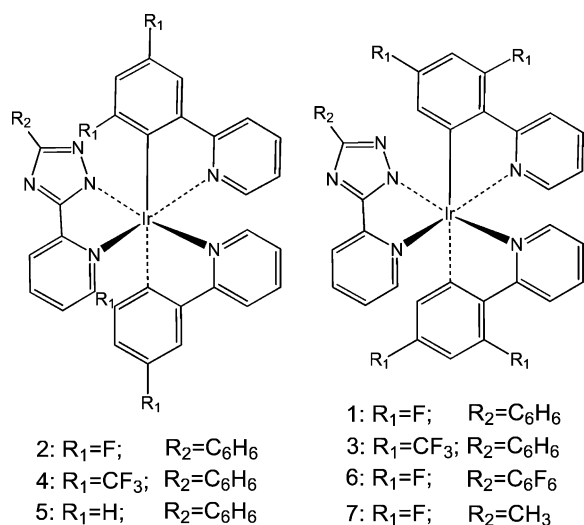
<sup>†</sup> Université de Mons-Hainaut.

<sup>‡</sup> Westfälische Wilhelms Universität Münster.

- (1) Baldo, M. A.; O'Brien, D. F.; You, Y.; Shoustikov, A.; Sibley, S.; Thompson, M. E.; Forrest, S. R. *Nature* **1998**, *395*, 151–154.
- (2) O'Brien, D. F.; Baldo, M. A.; Thompson, M. E.; Forrest, S. R. *Appl. Phys. Lett.* **1999**, *74*, 442–444.
- (3) Cleave, V.; Yahioglu, G.; Le Barny, P.; Friend, R.; Tessler, N. *Adv. Mater.* **1999**, *11*, 285–288.
- (4) Baldo, M. A.; Lamansky, S.; Burrows, P. E.; Thompson, M. E.; Forrest, S. R. *Appl. Phys. Lett.* **1999**, *75*, 4–6.
- (5) Tamayo, A. B.; Alleyne, B. D.; Djurovich, P. I.; Lamansky, S.; Tsyba, I.; Ho, N. N.; Bau, R.; Thompson, M. E. *J. Am. Chem. Soc.* **2003**, *125*, 7377–7387.
- (6) Dedeian, K.; Shi, J.; Shepherd, N.; Forsyth, E.; Morton, D. C. *Inorg. Chem.* **2005**, *44*, 4445–4447.
- (7) Song, Y.-H.; Yeh, S.-J.; Chen, C.-T.; Chi, Y.; Liu, C.-S.; Yu, J.-K.; Hu, Y.-H.; Chou, P.-T.; Peng, S.-M.; Lee, G.-H. *Adv. Funct. Mater.* **2004**, *14*, 1221–1226.

- (8) Grushin, V. V.; Herron, N.; LeCloux, D. D.; Marshall, W. J.; Petrov, V. A.; Wang, Y. *Chem. Commun.* **2001**, 1494–1495.
- (9) Tsuzuki, T.; Shirasawa, N.; Suzuki, T.; Tokito, Sh. *Adv. Mater.* **2003**, *15*, 1455–1458.
- (10) Coppo, P.; Plummer, E. A.; De Cola, L. *Chem. Commun.* **2004**, 1774–1775.
- (11) Hwang, F.-M.; Chen, H.-Y.; Chen, P.-S.; Liu, C.-S.; Chi, Y.; Shu, C.-F.; Wu, F.-L.; Chou, P.-T.; Peng, S.-M.; Lee, G.-H. *Inorg. Chem.* **2005**, *44*, 1344–1353.
- (12) Kwon, T.-H.; Cho, H. S.; Kim, M. K.; Kim, J.-Wh.; Kim, J.-J.; Lee, K. H.; Park, S. J.; Shin, I.-S.; Kim, H.; Shin, D. M.; Chung, Y. K.; Hong, J.-I. *Organometallics* **2005**, *24*, 1578–1585.
- (13) Yang, C.-H.; Li, S.-W.; Chi, Y.; Cheng, Y.-M.; Yeh, Y.-S.; Chou, P.-T.; Lee, G.-H.; Wang, C.-H.; Shu, C.-F. *Inorg. Chem.* **2005**, *44*, 7770–7780.
- (14) Mak, Ch. S. K.; Hayer, A.; Pascu, S. I.; Watkins, S. E.; Holmes, A. B.; Köhler, A.; Friend, R. H. *Chem. Commun.* **2005**, 4708–4710.
- (15) Li, J.; Djurovich, P. I.; Alleyne, B. D.; Yousufuddin, M.; Ho, N. N.; Thomas, J. C.; Peters, J. C.; Bau, R.; Thompson, M. E. *Inorg. Chem.* **2005**, *44*, 1713–1727.

Chart 1



appears to be responsible for larger Stokes shifts between the absorption and emission maxima and to give rise to weakly structured emission spectra.<sup>16–18</sup> We will show that the LC/MLCT ratio can be modulated by grafting electron-active substituents that change the localization of the triplet excitons in heteroleptic complexes containing chromophoric ligands of different natures.

While there is a large number of experimental papers addressing the photophysical properties of Ir(III)-based phosphorescent emitters,<sup>5–21</sup> there are still only a few corresponding theoretical studies.<sup>19,22</sup> Quantum-chemical calculations offer great possibilities in elucidating the structural and electronic properties of both the ground and excited states of transition metal complexes. In the present paper, we present a detailed theoretical and experimental study of the electronic properties of a series of Ir(III)-based complexes with three chromophoric ligands. The ligands are systematically two phenylpyridine (ppy) derivatives and one 2-(5-phenyl-4H-[1,2,4]triazol-3-yl)pyridine (ptpy) derivative (see Chart 1).

The concept of emission color tuning by grafting electron-active substituents relies on the fact that the lowest excited state is often relatively well described as a HOMO to LUMO transition in a given ligand. This promotes a good correlation between the HOMO–LUMO energy gap (measured as the difference between the ionization and reduction potentials) and the emission energy (see for example refs 23 and 24). Grafting electroactive groups at different positions of the ligands will, in general, change the HOMO–LUMO gap and, consequently, the emission energy. In order to tune the emission wavelength

over the whole visible range, it is highly desirable to find a way to modify the HOMO and LUMO energies independently.

When the molecular complex possesses different chromophoric ligands, some caution is required in determining the “optical” HOMO–LUMO gap, i.e., the gap between the orbitals involved in the lowest energy electronic transition. For example, according to DFT calculations performed on heteroleptic Ir complexes containing phenylpyrazole (ppz) and isoquinolinecarboxylic acid (iq) ligands, the HOMO and LUMO levels are localized on different ligands.<sup>12</sup> The authors of ref 12 came to the conclusion that this localization pattern gives the possibility of tuning the energies of the HOMO and LUMO levels independently, thus allowing for easier emission color tuning; this further implies that the emissive state should be a ligand-to-ligand charge transfer (LLCT) state. However, in another recent theoretical paper by Polson et al.<sup>19</sup> investigating a heteroleptic complex of Ir(III) with two different tridentate ligands (terpyridine (tpy) and diphenylpyridine (dppy)), the lowest triplet state has been found to be mostly tpy-centered and to contain only a small (~20%) admixture of LLCT character (dppy → tpy) despite the fact that the HOMO was mostly localized on dppy and the LUMO was fully localized on tpy.

Complexes 1–7 in our study are also made of two types of chromophoric ligands. The emissive triplet state may be localized on any of them, which could imply different photophysical properties among the various complexes. This has motivated a detailed theoretical analysis of the impact of substituents on the frontier molecular orbitals (MOs) localized on the phenylpyridine and ptpy ligands. We have found that the modification of the electronic structure of the ppy and ptpy ligands not only leads to the modulation of the energy of the lowest triplet excited state but also may further change the ordering of the lowest excited states, thus affecting the photophysical properties of the complexes.

## 2. Theoretical Methodology

Density functional theory (DFT) using Becke’s three-parameter hybrid functional B3LYP<sup>25,26</sup> was used for all calculations. The unrestricted B3LYP (UB3LYP) formalism was used for the geometry optimizations in the triplet state, while the calculations in the ground state were performed at the restricted level (B3LYP). Geometry optimizations were performed without any constraint. Spin contamination due to the admixture of excitations of higher multiplicity was rather small: the expectation values of spin operator  $\langle S^2 \rangle$  were below 2.03 for all triplet states. All calculations were performed using the split-valence 6-31G basis set for the ligands and the Hay–Wadt Los Alamos National Laboratory relativistic effective core potential and the LANL2DZ basis for Ir,<sup>27</sup> as implemented in Gaussian98 and Gaussian03.<sup>28</sup> The  $S_0 \rightarrow S_n$  transition energies were calculated with the time-dependent density functional theory (TD-DFT).<sup>29,30</sup> The  $S_0-T_1$  energy gaps were calculated by using both the TD-DFT and  $\Delta$ SCF approaches. The  $\Delta$ SCF method consists of approximating the  $S_0-T_1$  energy by taking the difference between the energies of the structures optimized in the ground and excited triplet state. TD-DFT calculations were performed on the basis of structures optimized in their ground state.

- (16) Colombo, M. G.; Hauser, A.; Güdel, H. U. *Inorg. Chem.* **1993**, *32*, 3081–3087.  
 (17) Colombo, M. G.; Brunold, T. C.; Hauser, A.; Güdel, H. U.; Förtsch, M.; Bürgi, H.-B. *Inorg. Chem.* **1994**, *33*, 545–550.  
 (18) Colombo, M. G.; Hauser, A.; Güdel, H. U. In *Topics in Current Chemistry: Yersin, H., Ed.; Electronic and Vibronic Spectra of Transition Metal Complexes I*; Springer: Berlin/Heidelberg, 1994; Vol. 171, pp 143–171.  
 (19) Polson, M.; Fracasso, S.; Bertolasi, V.; Ravaglia, M.; Scandola, F. *Inorg. Chem.* **2004**, *43*, 1950–1956.  
 (20) Lamansky, S.; Djurovich, P.; Murphy, D.; Abdel-Razzaq, F.; Kwong, R.; Tsyba, I.; Bortz, M.; Mui, B.; Bau, R.; Thompson, M. E. *Inorg. Chem.* **2001**, *40*, 1704–1711.  
 (21) Tamayo, A. B.; Garon, S.; Sajoto, T.; Djurovich, P. I.; Tsyba, I. M.; Bau, R.; Thompson, M. E. *Inorg. Chem.* **2005**, *44*, 8723–8732.  
 (22) Hay, P. J. *J. Phys. Chem. A* **2002**, *106*, 1634–1641.  
 (23) Pohl, R.; Anzenbacher, P., Jr. *Org. Lett.* **2003**, *5*, 2769–2772.  
 (24) Montes, V. A.; Pohl, R.; Li, G.; Shinar, J.; Anzenbacher, P., Jr. *Adv. Mater.* **2004**, *16*, 2001–2003.

- (25) Becke, A. D. *J. Chem. Phys.* **1993**, *98*, 5648–5652.  
 (26) Lee, C.; Yang, W.; Parr, R. G. *Phys. Rev. B* **1988**, *37*, 785–789.  
 (27) Hay, P. J.; Wadt, W. R. *J. Chem. Phys.* **1985**, *82*, 299–310.  
 (28) Frisch, M. J., et al. *Gaussian 98*, revision A.11; *Gaussian 03*, revision C.02; Gaussian, Inc.: Wallingford, CT, 2004.  
 (29) Casida, M. E.; Jamorski, C.; Casida, K. C.; Salahub, D. R. *J. Chem. Phys.* **1998**, *108*, 4439–4449.  
 (30) Stratmann, R. E.; Scuseria, G. E.; Frisch, M. J. *J. Chem. Phys.* **1998**, *109*, 8218–8224.

**Table 1.** Sum of the Mulliken Charges on the Carbon and Nitrogen Atoms of the Ligands for Complexes 1–7<sup>a</sup>

complex	Mulliken charge		
	phenylpyridine 1	phenylpyridine 2	ptpy
<b>1</b>	-0.66 (-0.74)	-0.57 (-0.74)	-1.78 (-0.01)
<b>2</b>	-0.62 (-0.78)	-0.54 (-0.77)	-1.78 (-0.01)
<b>3</b>	-1.16 (-0.24)	-1.06 (-0.25)	-1.77 (-0.02)
<b>4</b>	-1.11 (-0.29)	-1.02 (-0.29)	-1.77 (-0.02)
<b>5</b>	-1.40 (0)	-1.31 (0)	-1.79 (0)

<sup>a</sup> The charge withdrawn in comparison to the unsubstituted complex **5** is shown in parentheses.

### 3. Results and Discussion

**3.1. Nature of the Frontier Molecular Orbitals.** The influence of a particular substituent on an aromatic system is usually discussed in terms of inductive and mesomeric effects. The mesomeric effect is related to the sharing of  $\pi$ -electrons between the aromatic core and the substituent. If the substituent is grafted at a position where a frontier molecular orbital of the molecule has a node, its impact on this particular MO will be weak. If there is a significant electron density at the point of attachment, the interaction between the  $\pi$ -orbitals of the substituent and of the aromatic core is stronger, especially when the MOs are in resonance, i.e., when the energy gap between them is small.

The inductive effect is usually associated solely with the  $\sigma$ -electron system of the aromatic molecule. Electroactive groups that withdraw electron density by the inductive effect cause a lowering of the energies of the highest occupied and lowest unoccupied  $\pi$ -MOs. This can be explained qualitatively by the fact that electron acceptors withdraw some electron density from the ligands, thus reducing the repulsive Coulomb interaction between the electrons occupying the ligand-localized  $\pi$ -MOs and the electrons of the  $\sigma$ -system. The results of the present calculations indicate that the shape of the frontier  $\pi$ -MOs is important even with respect to substituents exerting mostly an inductive effect (*vide infra*).

We have examined the impact of fluorine and trifluoromethyl substituents in our systems by comparing the electron distribution in complexes 1–4 with respect to that of complex 5 which has no electron-withdrawing group (see Chart 1). The calculated Mulliken charges on the skeleton of the phenylpyridine and ptpy ligands are listed in Table 1. In comparison to complex 5, the CF<sub>3</sub> groups withdraw  $\sim 0.25$  |e| from each ppy ligand when added to positions 3 and 5 (complex 3) and  $\sim 0.29$  |e| when added to positions 2 and 4 (complex 4). At the same time, fluorine substituents withdraw  $\sim 0.75$  |e| from each ppy ligand in complexes 1 and 2. The Mulliken charges on the individual carbon atoms of the phenylpyridine ligands in complexes 1–5 are listed in Table 2. The charge distribution indicates that the charge is withdrawn locally, i.e., mostly from the atoms to which the electron acceptors are attached; as a result, the energies of the MOs that have large LCAO (linear combination of atomic orbitals) coefficients on these atoms should change to a larger extent.

Although the mesomeric and inductive effects are largely local (less so for the mesomeric effect), each of these two contributions strongly impacts the energy of the frontier orbitals and hence the electronic structure of the Ir complex. Note also that geometric distortions induced by the bulky trifluoromethyl substituents in complexes 3 and 4 might also alter the electronic

**Table 2.** Mulliken Point Charges on Selected Carbon Atoms of the Phenylpyridine Ligand and on Iridium for Complexes 1–5<sup>a</sup>

atom	Mulliken charge				
	complex 1 (F)	complex 2 (F)	complex 3 (CF <sub>3</sub> )	complex 4 (CF <sub>3</sub> )	complex 5
Ir	0.975	1.032	1.001	0.997	0.954
C1	-0.141	-0.172	-0.176	-0.052	-0.129
C2	-0.266	<i>0.174</i>	-0.206	<i>-0.184</i>	-0.247
C3	<i>0.330</i>	-0.149	<i>0.014</i>	-0.088	-0.088
C4	-0.189	<i>0.268</i>	-0.152	<i>-0.044</i>	-0.161
C5	<i>0.282</i>	-0.121	<i>0.004</i>	-0.087	-0.099
C6	0.004	0.012	0.029	-0.011	0.006

<sup>a</sup> The nature of the substituents is indicated in parentheses. Numbers in italics denote the Mulliken charges on carbon atoms to which the electron-withdrawing substituents are attached. The labeling of the atoms is shown in Figure 1.

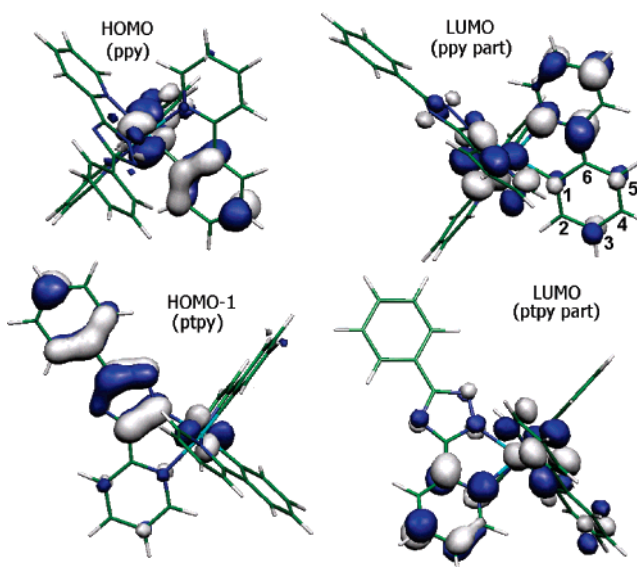


**Figure 1.** Contour plots of the frontier MOs of complex 5. The color and size of the lobes reflect the sign and amplitude of the LCAO coefficients, respectively. Two different views are shown for the LUMO, which is delocalized over both the ppy and ptpy ligands.

structure of the molecules. Although the task of quantifying and ranking each of these effects (geometric, mesomeric, and inductive) is not straightforward, it is possible to single out the most important effect in each complex.

Table 1 shows that fluorine atoms (complexes 1 and 2) are stronger electron-withdrawing substituents than trifluoromethyl groups (complexes 3 and 4). However, one must keep in mind that the fluorine substituents exert both inductive and mesomeric effects. In all complexes, the frontier MOs are localized mostly on either ppy or ptpy, with the exception of complex 5 in which the lowest unoccupied MOs of ptpy and one of the ppy ligands have nearly the same energy and are thus almost equally delocalized over them (see Figure 1). The electronic splitting resulting from this interaction is only on the order of 0.07 eV, thus demonstrating that the interaction between the orbitals is weak. The symmetries of the frontier MOs are similar in all complexes.

In view of the weak interactions between orbitals centered on different ligands, we now examine separately complexes 1–4 where electron-withdrawing substituents are added onto the ppy ligands and complexes 6 and 7 where the ptpy ligand is modified. Let us first focus on the ppy-localized frontier orbitals. The HOMO is mostly localized on the phenyl part of the phenylpyridine ligand and has a large contribution arising from

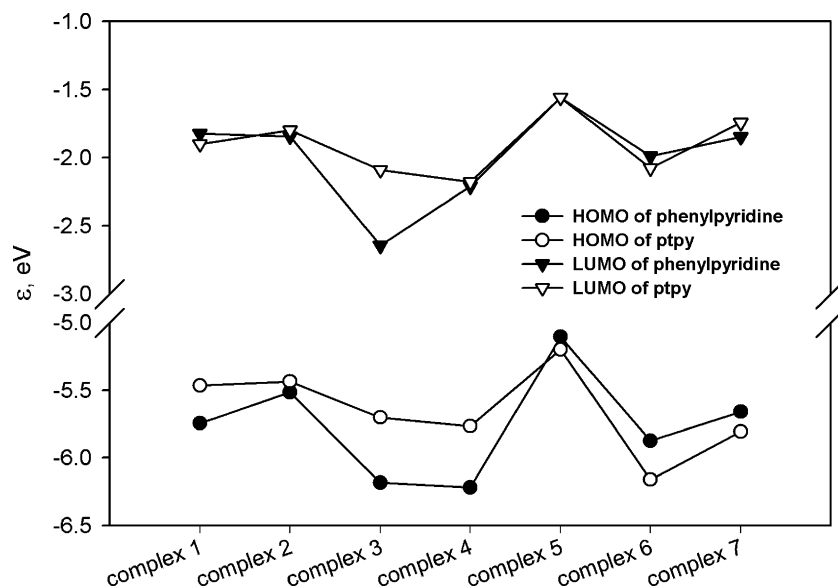


**Figure 2.** Energies of the frontier MOs localized either on ppy (● and ▼ for the HOMO and LUMO, respectively) or ptpy (○ and ▽ for the HOMO and LUMO, respectively).

the d atomic orbitals (AOs) of Ir (~40% according to the Mulliken population analysis), while the LUMO is mostly localized on the pyridine. The HOMO has large LCAO coefficients in positions 2 and 4 (and nodes in positions 3 and 5), whereas the opposite prevails for the LUMO level.

On the basis of the LCAO pattern of the frontier orbitals, it is possible to formulate the following rules of thumb to describe the influence of fluorine and trifluoromethyl substituents, when added to the phenyl part of the phenylpyridine ligand:

- The energy of the HOMO level will be more affected than the energy of the LUMO level since the latter is mostly centered over the pyridine ring;

- Substituents will perturb the HOMO energy to a larger extent (by both inductive and mesomeric effects) when added to positions 2 and 4. The impact of the substituents on the LUMO energy will be larger when they are grafted in positions 3 and 5.

Changing the substituents modifies the gap between the frontier orbitals localized on the different types of ligands (ppy and ptpy) and may even reverse their ordering, as illustrated in Figure 2. According to the calculations, the HOMO is localized on the ptpy ligand in complexes 1–4 and on the ppy ligands in complexes 5–7. The energy gap between the ppy- and ptpy-localized LUMOs is rather small for all complexes, except for complex 3 in which the ppy-localized LUMO lies 0.55 eV below the ptpy-localized LUMO. Differences in the localization of the frontier MOs are reflected in the cyclic voltammetry measurements, *vide infra*.

These rules rationalize the evolution of the energy gap between the frontier orbitals localized on ppy for complexes 1–5 (curve 3 in Figure 3A). In complex 3, the electron-accepting CF<sub>3</sub> groups are added in positions 3 and 5, which should lead to a strong decrease in the energy of the LUMO. However, since the charge is withdrawn not exclusively from positions 3 and 5, the fact that the LUMO is localized on the phenyl only to a small extent leads to a larger stabilization of the HOMO level and to an energy gap for complex 3, which is only marginally smaller than that of the unsubstituted complex 5. The addition of CF<sub>3</sub> groups at positions 2 and 4 (complex 4)

leads to a stronger stabilization of the HOMO according to the previous rules. Indeed, the calculated HOMO–LUMO gap for the ppy-localized orbitals of complex 4 increases by ~0.5 eV with respect to complex 5. The addition of fluorine atoms at positions 3 and 5 (complex 1) and positions 2 and 4 (complex 2) induces a stabilization of the frontier MOs; the HOMO is more stabilized, thus leading to an increase in the HOMO–LUMO gap of the ppy ligand by 0.38 and 0.13 eV for complexes 1 and 2, respectively, in comparison to complex 5. The peculiarity of fluorine as a substituent lies in the fact that, in addition to the strong inductive effect, its atomic p-orbital has the right energy to interact significantly with the frontier  $\pi$ -orbitals via a mesomeric effect. This interaction is stronger for the HOMO since its energy is closer to that of the 2p-atomic orbitals (AOs) of the fluorine atoms. The larger destabilization of the HOMO in complex 2 compared to complex 1 is explained by the fact that the fluorine atoms are added in complex 2 in positions 2 and 4, where the electron density is larger.

It is convenient to compare the electronic structure of complexes 6 and 7 to that of complex 1 since they all contain phenylpyridine ligands with fluorine atoms in positions 3 and 5. The LCAO pattern of the frontier orbitals localized on ptpy (Figure 1) is essentially the same for complexes 1 and 5. The HOMO is to a large extent delocalized over the triazol and phenyl rings while the LUMO is mostly localized on the pyridine ring. Note that there is an antibonding character over the bond connecting the phenyl and triazol rings in the ligand (Figure 1). The addition of fluorine atoms on the phenyl ring in complex 6 leads to a strong stabilization of the HOMO (by ~0.70 eV) with respect to the HOMO of complex 1 while the LUMO is stabilized to a smaller extent (~0.25 eV). The removal of the phenyl ring in complex 7 also leads to a stabilization of the HOMO level (by ~0.34 eV) with respect to the HOMO of complex 1 while leaving the energy of the LUMO almost unaffected. The stabilization of the HOMO level is attributed to the reduction of the antibonding character between the phenyl and triazol rings. In complex 6, the pentafluorination disrupts the coplanarity of the phenyl and triazol rings introducing a dihedral angle of ~45° between the two rings. Thus, the

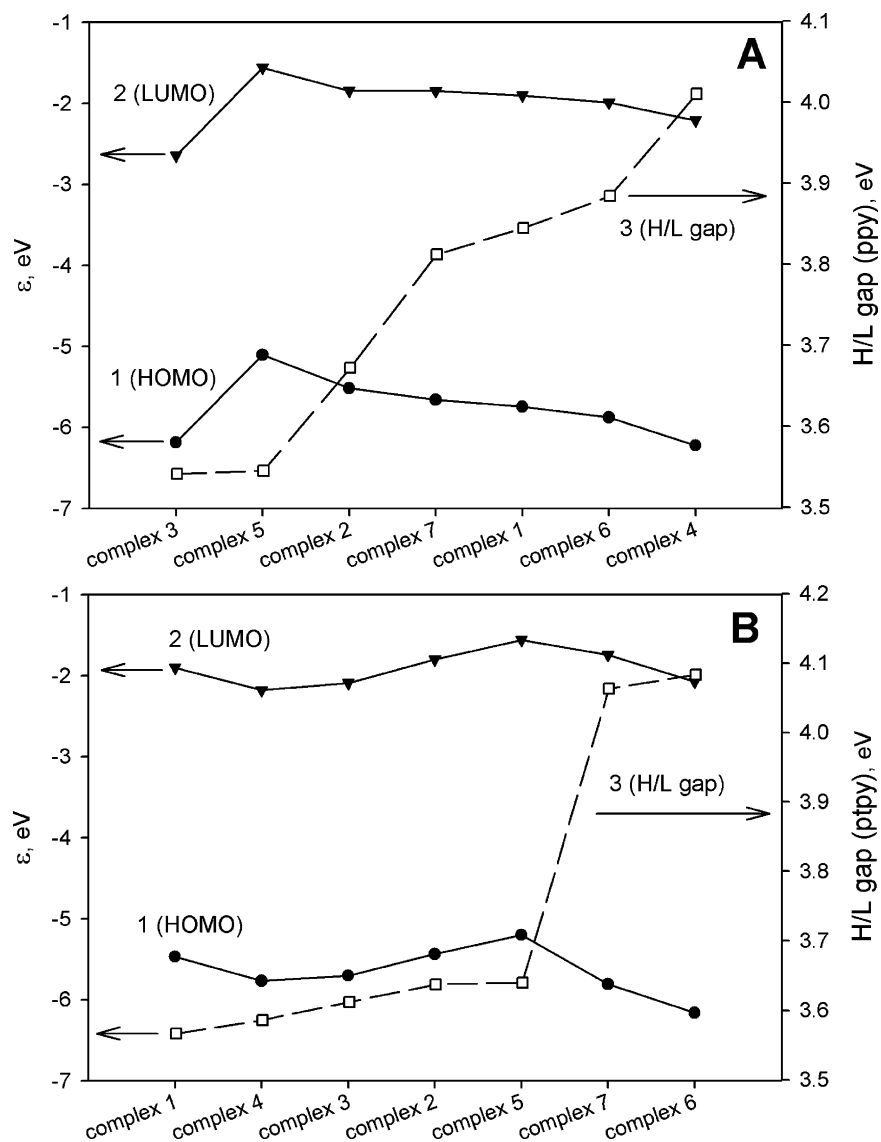


**Figure 3.** Energies of the frontier MOs, localized either on ppy (curves 1 and 2 in A) or ptpy (curves 1 and 2 in B) and HOMO–LUMO gaps for ppy (curve 3 in A) and ptpy (curve 3 in B).

structural changes introduced in the ptpy ligand in complexes **6** and **7** lead to a significant increase of the gap between the ptpy-localized frontier MOs compared to the other complexes (see Figure 3B).

The derivatization of the ppy ligand across the series **1–5** has little effect on the gap between the ppy-localized MOs, although the absolute values of the orbital energies vary among the complexes. Changes in electrostatic interactions upon derivatization of the ppy ligands are most likely responsible for this effect. Similarly, the gap between the ppy-localized MOs has almost the same value for complexes **1**, **6**, and **7**, which have the same ppy ligands.

**3.2. Cyclic Voltammetry Measurements.** Cyclic voltammetry (CV) has been used as an interrogator of the localization of the HOMO and LUMO levels in coordination complexes. Redox potentials that are similar in magnitude to those of the metal center or the ligands have been interpreted as indicators of whether the electronic process is centered on the metal or ligand, respectively. This assumption is reasonable since oxidation in coordination complexes is frequently associated with the process of removing an electron from a nonbonding d-orbital,

and reduction is frequently the addition of an electron to a LUMO that is mostly ligand-like by virtue of poor mixing with metal d-orbitals.<sup>11,13,15,20,21</sup> A considerable body of theoretical calculations shows that this association becomes tenuous for the cyclometalated complexes of Ir(III), where the HOMO is localized to a large extent on the ligands.<sup>6,12,15,22</sup> This facilitates the tuning of the electronic (spectroscopic) properties of these complexes over a wide energy range.

It is of prime interest to compare the values of ionization potential (IP) measured by cyclic voltammetry to the theoretical values obtained using Koopman's theorem, that is, the energies of the HOMO taken with a negative sign. Figure 4 shows a remarkable agreement between the theoretical and experimental values. Complexes **1**, **5**, and **6** exhibited reversible oxidation<sup>31</sup> while all the other complexes show almost irreversible oxidation. The oxidation potentials have been estimated for complexes **1**, **5**, and **6** as the average value of the peak maximum in the forward and reverse scans; when the oxidation is irreversible, the oxidation potentials reported in Figure 4 correspond to the

(31) Orselli, E.; Kottas, G. S.; Konradsson, A.; Coppo, P.; Fröhlich, R.; De Cola, L.; van Dijken, A.; Buechel, M.; Boerner, H., submitted.

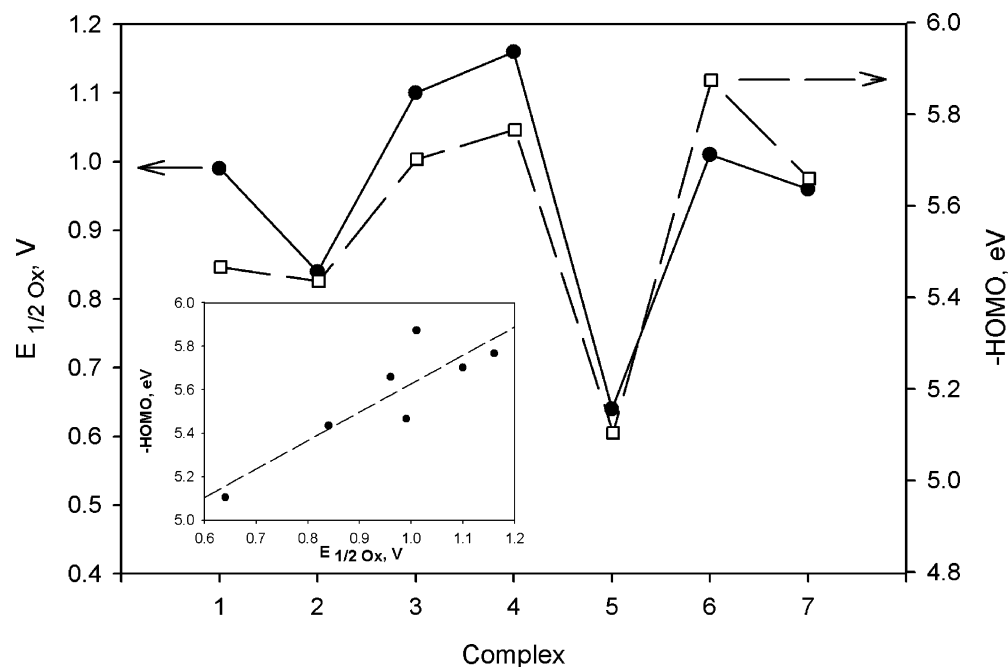


**Figure 4.** Half-wave oxidation potentials (measured in anhydrous, freshly distilled butyronitrile, and reported against the redox couple  $\text{Cp}_2\text{Fe}/\text{Cp}_2\text{Fe}^+$  used as internal standard; ●, full line) and calculated ionization potentials obtained by Koopman's theorem (□, dashed line). The inset shows a linear fit between the experimental and theoretical data.

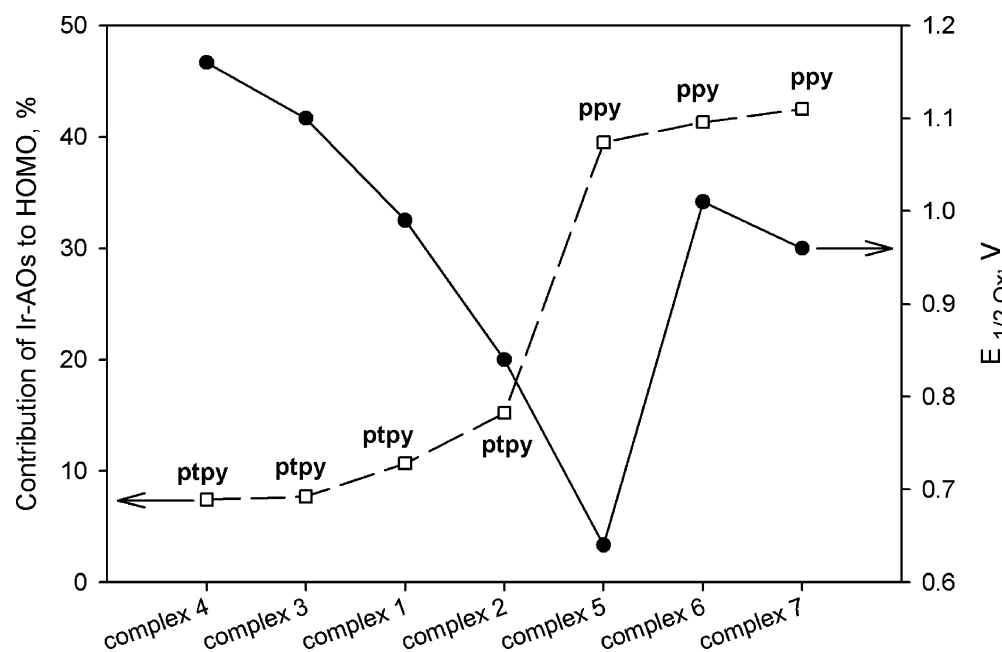


**Figure 5.** Calculated contribution of the d-atomic orbitals of iridium in the HOMO level (□, dashed line) and experimental oxidation potential (●, solid line) of complexes 1–7. The ligand on which the HOMO is mostly localized (ptpy or ppy) is also indicated.

peak maximum in the forward scan (this introduces an uncertainty on the values on the order of 30 meV). In the same way, the reduction for most of the complexes under study was not fully reversible except for complexes 6 and 3.<sup>31</sup> Complex 3 exhibited noteworthy reduction behavior with multiple waves at  $-1.4$ ,  $-1.8$ ,  $-2.0$ , and  $-2.2$  V. The quantum-chemical calculations suggest that reduction in complex 3 could be different from reduction in the other complexes since its ppy-centered LUMO is well separated in energy from the ptpy-localized unoccupied MOs.

The weight of the d-atomic orbitals of Ir in the description of the HOMO level varies significantly among the complexes

considered in this paper. According to our calculations, the contribution of such orbitals is always larger for the MOs which are mostly localized on the ppy-ligands (Figure 5). There is a clear anticorrelation between the contribution of the d-AOs of iridium and the oxidation potential for compounds 1–5: the larger the contribution from Ir, the smaller the oxidation potential. This does not hold true for complexes 6 and 7 whose HOMOs have the largest contribution from d-AOs of iridium, but whose oxidation potentials are approximately the same as that of complex 1. The discrepancy may be explained by the structural differences between complexes 1–5 and complexes 6 and 7. Complexes 1–5 form a homologous series with

derivatization on ppy, whereas **6** and **7** are homologues of **1** with derivatization on ptpy.

**3.3. Nature of the Lowest Triplet Excited States.** The energies of the lowest excited triplet states can be obtained either from the TD-DFT formalism or via  $\Delta$ SCF calculations. Both methods have been used to study the excited-state properties of Ir complexes<sup>19,22</sup> and yielded a good agreement between experimental and theoretical data. The TD-DFT calculations provide vertical transition energies from the ground-state geometry that is described at the restricted level. In contrast, the  $\Delta$ SCF method accounts for geometry relaxation in the excited triplet state by estimating the energy of the 0–0 transition as the difference between the total energies of the structures optimized in the ground state (using the spin restricted formalism) and in the excited triplet state (using the spin unrestricted formalism). We stress that the TD-DFT formalism provides a multiconfigurational description of the excited states, whereas the  $\Delta$ SCF approach treats the excited triplet states by promoting one electron from one occupied MO to one unoccupied MO. The advantage of TD-DFT is to provide information about a large number of excited states in a single run while one has to perform a different calculation for each electronic configuration in the case of the  $\Delta$ SCF method. We will compare hereafter the results provided by the two different approaches.

The nature of the excited states can be analyzed along different lines. The spin density distribution provided by unrestricted DFT calculations can shed light onto the localization of the triplet wavefunction. Among the several approaches applicable to the TD-DFT results (see ref 32 for a recent review), we will use hereafter the approach based on so-called “natural transition orbitals” (NTOs), as described in detail in refs 32 and 33. This transformation of the initial basis of molecular orbitals yields for each excited state a limited number of dominant configurations that promote one electron between two natural transition orbitals. The relative importance of each pair of “natural transition orbitals” is reflected through the corresponding eigenvalue  $\lambda$ . The sum of  $\lambda$  for all NTO pairs is equal to the sum of the squared configuration interaction coefficients; the latter is close to one but deviates slightly from unity when de-excitations are significant.<sup>32</sup> When the largest CI configurations correspond to one-electron excitation to the same unoccupied level, the NTO approach describes the hole wavefunction as  $\phi_{hole} = \sum_a CI_a \chi_a$ , with  $\chi_a$  as the occupied orbital in the initial basis set and  $CI_a$  as the corresponding CI coefficient. In such a case, one pair of NTOs often accounts for more than 90% of a transition, thus facilitating the analysis. A similar approach is also efficient when all the dominant CI configurations correspond to excitations from the same occupied level.

The energies of the lowest excited triplet state provided by TD-DFT calculations for complexes **1–7** together with an illustration of the dominant pair of “natural transition orbitals” for some complexes are presented in Table 3. The values of  $\lambda$  reported in the last column are all close to unity and show that the NTO procedure is successful in describing the triplet excited states of the complexes under study. The triplet states can be classified in two categories: (i) states mostly characterized by an excitation of the phenylpyridine ligands which have a pronounced MLCT character due to the fact that the electron is

promoted from an orbital having a large contribution of the metal d-AOs; and (ii) states mostly characterized by an excitation of the ptpy ligand in which the participation of the atomic orbitals of iridium is considerably smaller. The TD-DFT calculations show that the ordering of the lowest triplet states of type (i) (ppy-centered) and type (ii) (ptpy-centered) and the energy gap between them varies from one complex to another. The lowest triplet excited state is centered on the ptpy ligand for **1**, **2**, and **4** while the  $T_2$  state of these complexes is mostly centered on one of the ppy ligands. On the contrary, the  $T_1$  state is mostly localized on one of the ppy ligands in complexes **5** and **7** while  $T_2$  corresponds to a local excitation of the ptpy ligand. In complex **6**, the lowest two triplet states are almost degenerate, both being localized on a given ppy ligand while the third triplet state is mostly ptpy centered. The lowest triplet states of complex **3** have a more complex nature: the  $T_1$  state is formed by a mixture of local excitations on ppy and by Ir  $\rightarrow$  ppy MLCT and ptpy  $\rightarrow$  ptpy LLCT excitations while the  $T_2$  state mostly originates from local excitations on the ptpy ligand with contributions from ptpy  $\rightarrow$  ppy LLCT and MLCT excitations.

The NTO procedure was more successful for complexes **1** and **4** and less applicable for complexes **5** and **7**. This is explained by the fact that the gap between the lowest ppy- and ptpy-localized triplet states is the largest for complexes **1** and **4**, thus preventing a mixing between the local excitations. In contrast, the ppy- and ptpy-localized triplet states are very close in energy in complexes **5** and **7**, thus leading to a partial mixing albeit relatively small; the energy gap between ppy- and ptpy-localized states is very small in complex **7** (on the order of 0.004 eV) indicating that the electronic coupling between the ligands is very small. By extension, such a small electronic coupling is likely to explain the dual luminescence from thermally non-equilibrated excited states that has been observed for [Ir-(ppy)<sub>2</sub>bpy]<sup>+</sup> complexes (bpy=2,2'-bipyridine).<sup>34,35</sup>

Variations in the weight of the MLCT and LLCT contributions in the description of the lowest singlet and triplet excited states lead to changes in the  $S_1$ – $T_1$  energy gap among the various complexes (Table 4); note that corresponding experimental values are not accessible since the high efficiency of the intersystem crossing processes (with a yield close to 1) makes the fluorescence signal hardly detectable for the iridium complexes under study. The singlet–triplet energy gap ( $\Delta E_{ST}$ ) reflects the amplitude of the exchange interactions, which depends, to a large extent, on the degree of electronic overlap between the occupied and unoccupied molecular orbitals involved in the  $S_0 \rightarrow S_1$  and  $S_0 \rightarrow T_1$  transitions. Thus, the gap between singlet and triplet excited states with a dominant MLCT and LLCT character is expected to be smaller than that associated with LC states due to the fact that the overlap between the occupied and unoccupied orbitals is small in the former case. Complexes **1**, **2**, and **4** have the smallest CT contributions in the lowest excited states and thus exhibit large singlet–triplet energy gaps ( $\Delta E_{ST} > 0.35$  eV). In contrast, the lowest excited states of complexes **5**, **6**, and **7** are characterized by a large admixture of MLCT excitations and yield a smaller  $\Delta E_{ST}$  (0.23–0.27 eV). The  $S_1$  and  $T_1$  states of complex **3** have large contributions arising from both MLCT and LLCT excitations; as a result, complex **3** has the smallest  $\Delta E_{ST}$  (0.08 eV).

(32) Dreuw, A.; Head-Gordon, M. *Chem. Rev.* **2005**, *105*, 4009–4037.

(33) Martin, R. L. *J. Chem. Phys.* **2003**, *118*, 4775–4777.

(34) King, K. A.; Watts, R. J. *J. Am. Chem. Soc.* **1987**, *109*, 1589–1590.

(35) Wilde, A. P.; King, K. A.; Watts, R. J. *J. Phys. Chem.* **1991**, *95*, 629–634.

**Table 3.** Contour Plots of the Pairs of “Natural Transition Orbitals” Contributing the Most to the Description of the Lowest Triplet Excited States of Complexes 1–7<sup>a</sup>

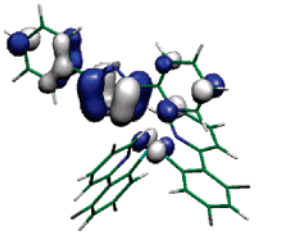
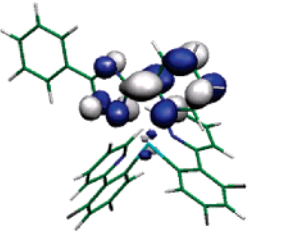
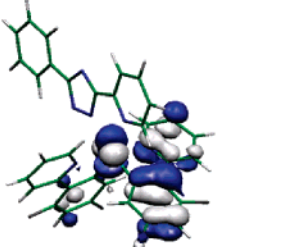
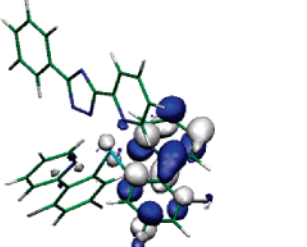
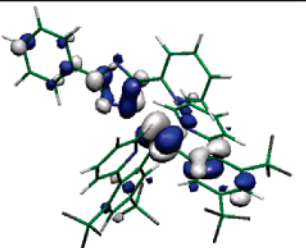
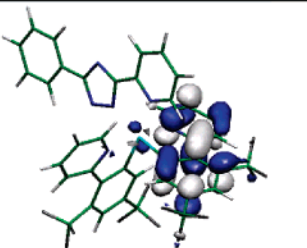
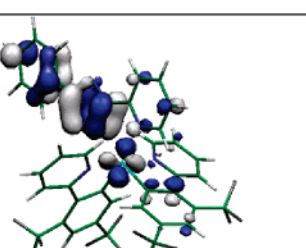
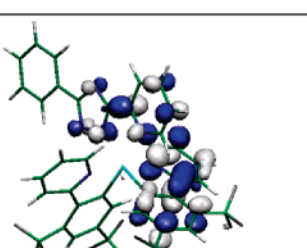
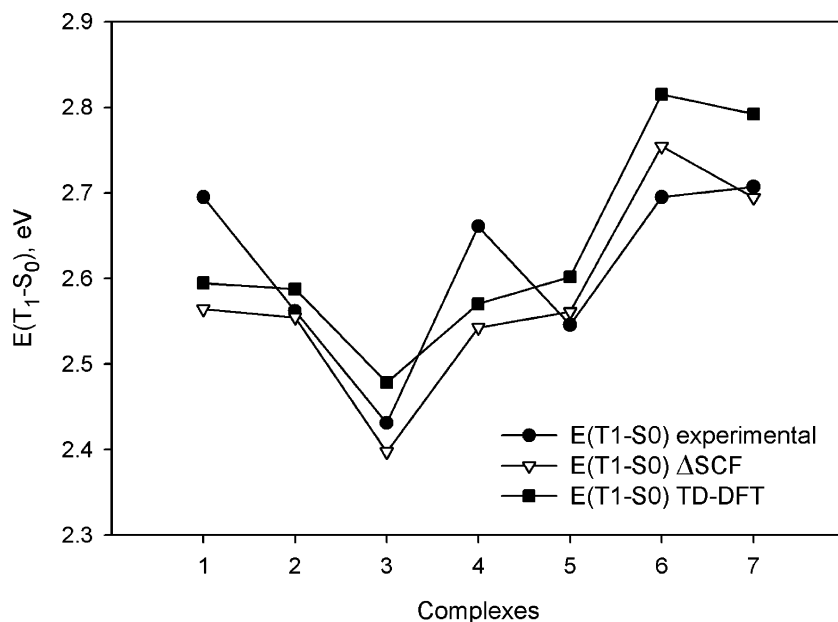
Excited state	E, eV	Occupied NTO	Unoccupied NTO	$\lambda$ / CI
Complex 1				
T <sub>1</sub>	2.59			1.12 / 1.15
T <sub>2</sub>	2.80			0.95 / 1.19
Complex 2				
T <sub>1</sub>	2.59	ptpy-localized		1.12 / 1.15
T <sub>2</sub>	2.68	ppy-localized		1.07 / 1.15
Complex 3				
T <sub>1</sub>	2.48			1.01 / 1.09
T <sub>2</sub>	2.56			0.97 / 1.11
Complex 4				
T <sub>1</sub>	2.57	ptpy-localized		1.12 / 1.16
T <sub>2</sub>	2.86	ppy-localized		1.01 / 1.26
Complex 5				
T <sub>1</sub>	2.60	ppy-localized		0.89 / 1.13
T <sub>2</sub>	2.61	ptpy-localized		0.93 / 1.15



Table 3 (Continued)

Complex 6			
T <sub>1</sub>	2.82	ppy-localized	1.00 / 1.20
T <sub>2</sub>	2.86	ppy-localized	0.99 / 1.24
T <sub>3</sub>	2.93	ptpy-localized	1.09 / 1.17
Complex 7			
T <sub>1</sub>	2.79	ppy-localized	0.77 / 1.18
T <sub>2</sub>	2.80	ptpy-localized	0.85 / 1.19

<sup>a</sup> The energies of the states are reported in the second column. The  $\lambda$  value quantifying the contribution of the NTO pair is reported in the last column. “CI” corresponds to the sum of the squared CI coefficients associated to all singly excited configurations contributing to the excited state. Since the shape of the orbitals for ppy or ptpy localized transitions is similar to that of complex 1 in most cases except for complex 3, we present the NTOs only for those two complexes (the other NTOs can be found in the Supporting Information).



**Figure 6.** Theoretical T<sub>1</sub>–S<sub>0</sub> transition energies calculated by TD-DFT (■) and ΔSCF (▽) compared to the experimental 0–0 T<sub>1</sub>–S<sub>0</sub> transition energies (estimated from the position of the highest energy peak of emission spectra recorded in spectroscopic grade dichloromethane at 293 K (10); ●) for complexes 1–7.

**Table 4.** TD-DFT-Calculated Values of the S<sub>1</sub>–T<sub>1</sub> Energy Gaps ( $\Delta E_{ST}$ ) in Complexes 1–7

complex	$\Delta E_{ST}$ , eV
1	0.40
2	0.35
3	0.08
4	0.46
5	0.23
6	0.28
7	0.27

In order to further explore the properties of the lowest triplet excited states, we performed geometry optimizations for complexes 1–7 at the spin-unrestricted B3LYP level. For each complex, we focus on two triplet states of different types: the lowest triplet state localized on ptpy (as revealed by the spin density distribution) and the lowest triplet state mostly localized on the ppy ligand. The geometry optimizations in these two

states are performed by choosing an appropriate initial electronic configuration.

Table 5 collects the net Mulliken charges transferred from (if positive) or to (if negative) a particular fragment of the complexes in the lowest triplet state with respect to the ground state charge distribution as well as the sum of Mulliken atomic spin densities over the different fragments, as provided by the B3LYP calculations. The contribution of MLCT excitations can be assessed either from the charge transferred from the iridium atom or from the value of the spin density on Ir. The MLCT contributions provided by the Mulliken charges in the lowest triplet state are smaller than those suggested by the shapes of the NTO orbitals at the TD-DFT level. In agreement with the NTO analysis of the TD-DFT results, ppy-localized triplet excited states exhibit the larger admixture of charge-transfer contributions; the maximum charge transferred from Ir is  $\sim 12\%$  of  $|e|$  in complex 5. The contributions from ligand-to-ligand

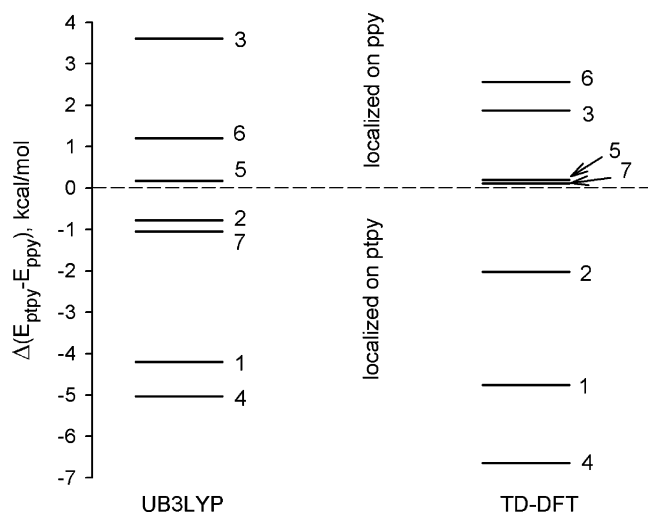


**Figure 7.** Energy difference between the ptpy- and ppy-localized triplet excited states for complexes 1–7, as predicted by the TD-DFT and  $\Delta$ SCF calculations. Negative values indicate that the lowest triplet state is localized on the ptpy ligand.

**Table 5.** Net Mulliken Charge Transferred from (if Positive) or to (if Negative) a Particular Fragment of the Complexes in the Lowest Triplet State with Respect to the Ground-State Charge Distribution (at the Restricted Level), as Well as the Sum of Mulliken Atomic Spin Densities over Different Fragments, as Calculated at the UB3LYP Level

complex (triplet localization)	Mulliken charge  e			Mulliken spin density  e		
	Ir	ptpy	ppy	Ir	ptpy	ppy
1 (ptpy)	0.031	−0.047	0.016	0.106	1.902	−0.009
2 (ptpy)	0.032	−0.057	0.025	0.121	1.888	−0.009
3 (ppy)	0.107	0.072	−0.179	0.394	0.045	1.561
4 (ptpy)	0.014	−0.031	0.017	0.089	1.924	−0.013
5 (ppy)	0.121	0.045	−0.166	0.384	0.017	1.599
6 (ppy)	0.085	0.030	−0.116	0.282	0.008	1.710
7 (ptpy)	0.034	−0.076	0.042	0.125	1.885	−0.009

CT excitations, estimated from the smallest charge transferred from or to one of the ligands, are even smaller; complex 3 has the largest LLCT contribution ( $\sim 7\%$ ), in agreement with the TD-DFT results. The Mulliken spin density distribution yields larger MLCT contributions (as estimated from the spin density on Ir) in the lowest triplet states compared to those predicted by the Mulliken charge distributions. Ptpy-localized triplet excited states have a small admixture of MLCT character ( $\leq 6\%$ ) while the MLCT contribution in the phenylpyridine-localized states is considerably larger (from 14 to 20%); similar trends are found at the TD-DFT level. That the spin density distribution better matches the results of the NTO analysis in comparison to the charge distribution can be explained in the following way: the spin distribution is mostly governed by the shape of the two frontier MOs (most often the HOMO and LUMO levels) that are involved in the lowest triplet excitation. In contrast, a change in the electrostatic potential occurs when exciting a state with a pronounced charge-transfer character, thus leading to a redistribution of the total electronic density (built from all occupied MOs).

The difference between the TD-DFT and  $\Delta$ SCF results is further governed by the tendency of the triplet wavefunction to get localized in the spin-unrestricted calculations which favor locally excited configurations and thus reduce the MLCT and

LLCT contributions.<sup>36–40</sup> Note, however, that there are fundamental differences between the two approaches since: (i) the  $\alpha$  and  $\beta$  electrons occupy different spatial orbitals in the spin-unrestricted DFT calculations performed for the triplet state, whereas the TD-DFT calculations are coupled to a restricted formalism; and (ii) the geometry is fully relaxed in the two states with  $\Delta$ SCF while TD-DFT deals with vertical excitations. The energies of the  $T_1 \rightarrow S_0$  transition, predicted by both the TD-DFT and  $\Delta$ SCF methods, are found to be in reasonably good agreement with the experimental 0–0  $T_1 \rightarrow S_0$  transition energies extracted from the emission spectra (see Figure 6) and to reproduce the experimental evolution among the various complexes.

Finally, it is of interest to compare the relative energies of the lowest triplet state mostly localized on either the ppy or ptpy ligand in the various complexes, as predicted by TD-DFT and UB3LYP calculations (see Figure 7). The ordering of the two states and their energy difference are similar when comparing the TD-DFT and  $\Delta$ SCF results. This does not hold true for complex 7, which has the two triplet states lying at almost the same energy. There is also a slight disagreement for complexes 6 and 3:  $\Delta$ SCF predicts the largest energy difference between ppy- and ptpy-localized states for complex 3, while, according to TD-DFT, it is the largest for complex 6. We believe that this disagreement is related to the different amounts of CT excitations in the description of the lowest triplet state of the complex 3 by  $\Delta$ SCF and TD-DFT. According to the  $\Delta$ SCF calculations, the energy gap between the ptpy- and ppy-localized triplet states is the largest for complexes 4, 1, and 3; the lowest energy state is localized on ptpy in 4 and 1 and on ppy in 3.

Changes in the nature of the lowest excited states among complexes 1–7 can be understood on a qualitative basis by considering the HOMO–LUMO gaps for transitions of different types, as illustrated in Figure 8. Figure 8A shows the correlation between the difference in the energy gaps between the frontier MOs of ppy and ptpy ligands and the localization of the lowest triplet excited state. One may see that, with the exception of complex 7, the triplet state is localized on the ligand which has the smaller energy gap between the corresponding frontier MOs (the lower left quadrant is associated with ptpy-localized triplet states while the upper-right quadrant refers to ppy-localized triplet states). Figure 8B shows the correlation between the admixture of inter-ligand CT character (estimated from the values of the Mulliken charges according to the  $\Delta$ SCF calculations, *vide supra*) in the lowest triplet excited state and the energy gap between the MOs involved in the corresponding CT excitation (when the triplet state is localized on ppy, the charge transfer occurs from ptpy to ppy and *vice versa*): the smaller the value of this gap with respect to the intramolecular gap of the ligand on which the triplet state is localized, the larger the admixture of CT character. For example, the energy difference between the highest occupied ptpy MO and the lowest

(36) Beljonne, D.; Cornil, J.; Brédas, J. L.; Friend, R. H.; Janssen, R. A. J. *J. Am. Chem. Soc.* **1996**, *118*, 6453–6461.

(37) Beljonne, D.; Cornil, J.; Brédas, J. L.; Friend, R. H. *Synth. Met.* **1996**, *76*, 61–65.

(38) Beljonne, D.; Wittmann, H. F.; Köhler, A.; Graham, S.; Younus, M.; Lewis, J.; Raithby, P. R.; Khan, M. S.; Friend, R. H.; Brédas, J. L. *J. Chem. Phys.* **1996**, *105*, 3868–3877.

(39) Dos Santos, D. A.; Beljonne, D.; Cornil, J.; Brédas, J. L. *Chem. Phys.* **1998**, *227*, 1–10.

(40) Avilov, I.; Marsal, P.; Brédas, J. L.; Beljonne, D. *Adv. Mater.* **2004**, *16*, 1624–1629.

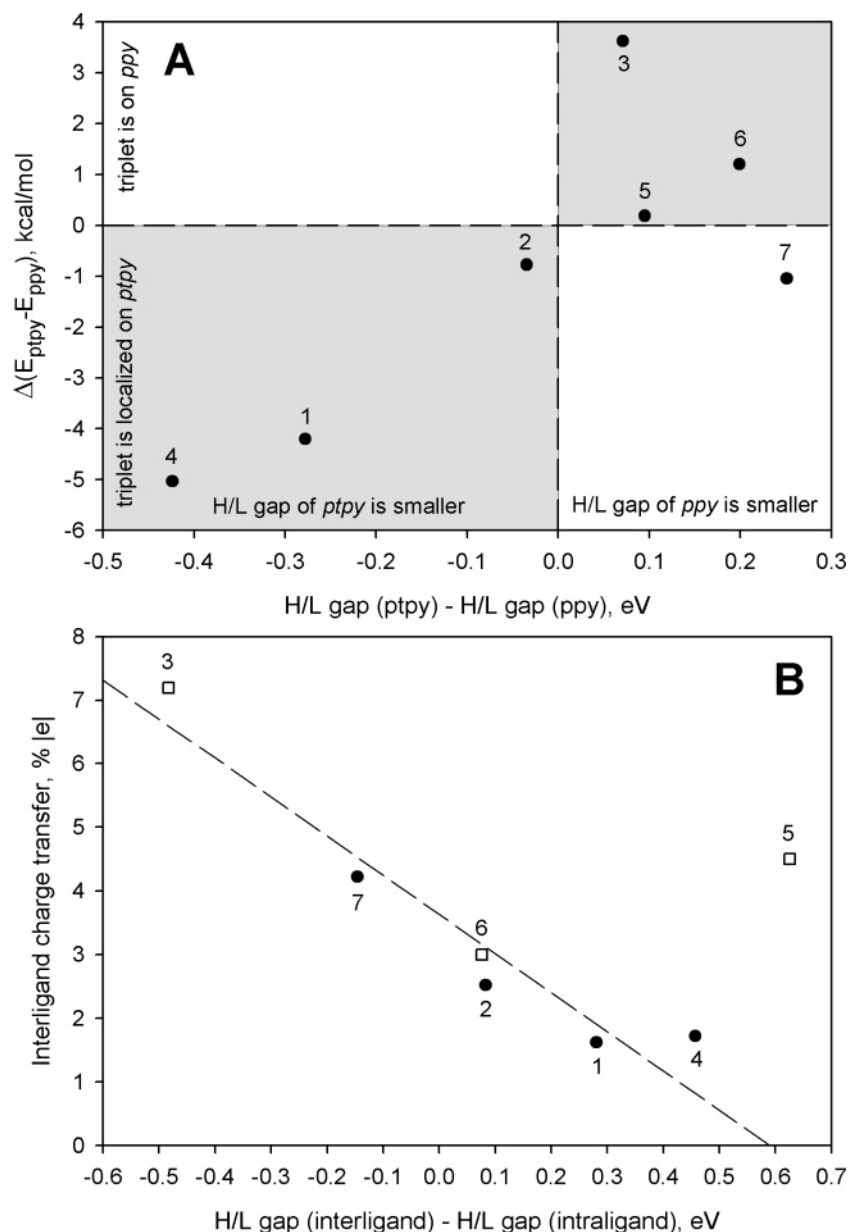


**Figure 8.** (A) Comparison between the HOMO/LUMO gaps for local excitations and the localization of the triplet state. The energy difference between the HOMO/LUMO gaps of ptpy and ppy ligands is plotted along the X axis. Negative values indicate that the HOMO/LUMO gap of the ptpy ligand is smaller than that of the ppy ligand. The energy difference between the ptpy- and ppy-localized triplet excited states, as predicted by  $\Delta$ SCF calculations, is plotted along the Y-axis. Negative values indicate that the lowest triplet state is localized on the ptpy ligand. (B) Comparison between the HOMO/LUMO gaps for inter-ligand excitations and the charge-transfer contribution to the lowest triplet state. The energy difference between HOMO/LUMO gaps for ptpy-to-ppy and ppy-to-ppy excitations (complexes 3, 5, and 6;  $\square$ ) and ppy-to-ptpy and ptpy-to-ptpy excitations (complexes 3, 5, and 6;  $\bullet$ ) is reported along the X axis. The dashed line is the linear fit of the data not including complex 5.

unoccupied ppy MO has the smallest value for complex 3 while the amount of charge transferred from the ptpy ligand to the ppy ligand is the largest. This is also consistent with the NTO analysis suggesting that LLCT excitations of ptpy  $\rightarrow$  ppy type play an important role in complex 3 (*vide supra*). A careful analysis of the relative energies of the frontier MOs can thus shed light onto the nature of the lowest excited states of the complexes under study.

#### 4. Conclusions

In summary, we have performed a detailed theoretical analysis of the influence of fluorine and trifluoromethyl substituents on the properties of the emissive state of a series of Ir(III) cyclometalated complexes. Our calculations reproduce and

rationalize the experimental redox and excited-state properties of the Ir complexes under study.

When a phosphorescent complex is made of different chromophoric ligands, special care should be taken when defining strategies for emission color tuning. The localization of the emissive state may vary as a function of the substitution pattern. The pair of occupied/unoccupied orbitals characterizing the different triplet excitations has to be identified, and the influence of the substituents on the energy gap of each of these pairs should be considered. The introduction of substituents not only modulates the emission energy but also often changes the ordering of the lowest excited triplet states and hence their localization.

Spin-unrestricted DFT calculations indicate that the lowest triplet state is more localized than suggested by TD-DFT calculations. The lowest triplet states are best characterized as local excitations of one of the chromophoric ligands (phenylpyridine or phenyl-triazol-pyridine). The admixture of MLCT and LLCT character is small and strongly depends on the nature of the excited state; their role is, however, primordial in defining the radiative decay rate of the complexes.

**Acknowledgment.** The work in Mons has been supported by the Belgian Federal Government “Interuniversity Attraction Pole in Supramolecular Chemistry and Catalysis, PAI 5/3”, the

European Commission through the Human Potential Programme (Marie-Curie RTN NANOMATCH, Grant No. MRTN-CT-2006-035884), and the Belgian National Fund for Scientific Research (FNRS/FRFC). J.C. is an FNRS Research Associate. The research in Münster was supported by Philips Research and SENTER (TRIPLED RWC-061-JH-04063-jh).

**Supporting Information Available:** Cartesian coordinates of all complexes optimized in their ground and lowest two triplet states; complete Table 3; complete ref 28. This material is available free of charge via the Internet at <http://pubs.acs.org>.

JA0711011